EPJ manuscript No.
(will be inserted by the editor)

Analysis of $(\pi^{\pm}, K^{+})$ and (K^{-}, K^{+}) hypernuclear production spectra in distorted wave impulse approximation

Hideki Maekawa, Kohsuke Tsubakihara and Akira Ohnishi

Department of Physics, Faculty of Science, Hokkaido University Sapporo 060-0810, Japan

Received: date / Revised version: date

Abstract. We study the hyperon-nucleus potential with distorted wave impulse wave approximation (DWIA) using Green's function method. In order to include the nucleon and hyperon potential effects in Fermi averaging, we introduce the local optimal momentum approximation of target nucleons. We can describe the quasi free Λ, Σ and Ξ production spectra in a better way than in the standard Fermi averaged t-matrix treatments.

PACS. 21.80.+a Hypernuclei – 24.50.+g Direct reactions

1 Introduction

Study of hyperon-nucleon (YN) interaction has an advantage that the contributions of meson and quark exchange are different from those in NN interaction, then it may give an opportunity to separate or distinguish them. For example, Λ does not couple with pions directly then the strength of the middle range central attraction would be different in meson and quark exchange pictures. The situation would be clearer for Σ hyperons. Due to the isovector nature of the diquark pair in Σ, the Pauli blocking effects between quarks appear in a more direct manner in ΣN interaction. The Σ potential in nuclear matter at saturation density is predicted to be around +30 MeV (repulsion) in a quark cluster model YN potential [1], while the potential is less repulsive or attractive in many of the hadronic YN potential models.

Hyperon potential in nuclear matter is also important to understand compact astrophysical objects such as neutron stars. The Λ hyperon-nucleus potential has been investigated in the bound region extensively, and its depth has been known to be about 30 MeV [2]. For Σ hyperon, the bound state spectroscopy is difficult, because of the strong Λ conversion, $\Sigma N \to \Lambda N$. In ${}^{4}_{\Sigma}$He, which is the only case of observed Σ (quasi) bound state [3], the coupling effects is strong and the repulsive contribution in the T =3/2, ${}^3S_1$ channel is suppressed, then it does not strongly constrain the Σ potential in nuclear matter. The analysis of Σ^- atomic data suggested a Σ^--nucleus potential having a shallow attractive pocket around the nuclear surface and repulsion inside the nucleus [4], but it is difficult to determine the Σ^--nucleus optical potential in the inner part of nucleus from the atomic data unambiguously.

Send offprint requests to: mae@nucl.sci.hokudai.ac.jp

One of the methods to evaluate the hyperon-nucleus potential is to analyze the quasi free (QF) spectrum in the continuum region [5]. Recent observation of inclusive (π^-,K^+) spectra on heavy nuclear targets performed at KEK [6] has made our understanding of Σ-nucleus potential a step forward. In the distorted wave impulse approximation (DWIA) analyses, it is suggested that the repulsive real potential of 90 MeV or more would be necessary to reproduce the experimental spectra [6]. Since this very repulsive Σ potential in nuclei cannot be supported by any theoretical models, it is necessary to verify the validity of approximations and prescriptions in the reaction theory currently used for the analysis. Recently, Harada and Hirabayashi pointed out that on-shell condition in Fermi averaging (optimal Fermi averaging) for t-matrix of elementary process is important to understand the shape of the QF spectrum [8], and their analysis suggests that Σ^--nucleus potential has the repulsive feature in the center of nuclei [9]. A Semi Classical Distorted Wave (SCDW) analysis by Kohno *et al.* [10] also suggests the repulsive nature. In these works, while the former is based on a fully quantum treatment, the nucleon and hyperon potential effects are included in the latter. If the on-shell condition is important and the difference of the initial (nucleon) and final (hyperon) potentials is large, it would be necessary to take account of the effects of the kinematics modification due to the potential energy in the on-shell condition of the elementary process in nuclear environment within a quantum mechanical framework in order to understand the hyperon production spectra in the QF and bound state region.

In this paper, we investigate the hyperon-nucleus potential through hyperon production spectra by introducing the local optimal Fermi averaging t-matrix in DWIA, which is expected to possess both of the merits in the previous two works.

2 Model; Green's function method and Local optimal Fermi averaged t-matrix

The Green's function method has been widely applied to the analysis of hypernuclear reactions. This method has the advantage to treat the continuum as well as bound state region on the same footing. In order to include the effects of nucleon Fermi motion and nucleon/hyperon potentials into optimal Fermi averaging t-matrix, we introduce the Local Optimal Fermi Averaging t-matrix (LOFAt).

Using the Fermi's golden rule, the differential cross section of (π, K) reaction is written as [11],

$$\frac{d^2\sigma}{dE_K d\Omega_K} = \frac{p_K E_K}{(2\pi\hbar^2)^2 v_\pi} \sum_f |T_{fi}|^2 \delta(E_\pi + E_T - E_K - E_H) \ , \tag{1}$$

where the subscripts T and H represent target and produced hypernucleus, respectively, and $v_\pi = p_\pi/E_\pi$ is the incident particle velocity.

From the angular momentum algebra, we can get the partial wave decomposition of the strength function $S(E)$ in the Green's function method [12],

$$\frac{d^2\sigma}{dE_K d\Omega_K} = \frac{p_K E_K}{(2\pi\hbar^2)^2 v_\pi} S(E) \ , \tag{2}$$

$$S(E) = \sum_{JM} \sum_{\alpha\beta} \sum_{\alpha'\beta'} W[\alpha\beta\alpha'\beta'] S^{JM}_{\alpha\beta\alpha'\beta'}(E) \ , \tag{3}$$

$$S^{JM}_{\alpha\beta\alpha'\beta'}(E) = -\frac{1}{\pi} \mathrm{Im} \int r^2 dr\, r'^2 dr' \tilde{j}^*_{JM}(r) \phi^*_\alpha(r) \bar{t}^*(r) \times G^{JM}_{\alpha\beta\alpha'\beta'}(E; r, r') \bar{t}(r') \tilde{j}_{JM}(r') \phi_{\alpha'}(r') \ . \tag{4}$$

Here subscripts α and β stand for the quantum numbers of nucleon and hyperon states, respectively. The coefficient $W[\alpha\beta\alpha'\beta']$ represents the hypernuclear statistical factor. The function $\tilde{j}_{JM}$ is called distorted Bessel function [13], $\phi_\alpha(r)$ is the radial wave function of target nucleon, and J is the total spin of hypernuclei. The Green's function $G_{\alpha\beta\alpha'\beta'}(E; r, r')$ contains the hypernuclear Hamiltonian H_H then we can get the information of optical potential U_Y between hyperon and nucleus.

It was pointed out by Harada and Hirabayashi [8] that on shell kinematics in the Fermi averaging procedure roughly decide the shape of the QF spectrum and its prescription of the t-matrix is important. We would like to extend their idea by including potential effects. Here, we introduce *Local Optimal Fermi Averaging* t-matrix (LOFAt),

$$\bar{t}(r; \omega, \boldsymbol{q}) \equiv \frac{\int d\boldsymbol{p}_N t(s,t) \rho(p_N) \delta^4(P^\mu_f(r) - P^\mu_i(r))}{\int d\boldsymbol{p}_N \rho(p_N) \delta^4(P^\mu_f(r) - P^\mu_i(r))} \ , \tag{5}$$

where $P^\mu_{i,f}(r)$ denote the total four momenta in the elementary initial and final two-body states. We adopt the Fermi distribution function for the target nucleon momentum distribution $\rho(p_N)$ and parameters are taken from [11, 14].

In obtaining LOFA t-matrix, we define the nucleon and hyperon energy in nuclei and hypernuclei containing the nuclear and hypernuclear potential effects,

$$E_B(r) = \sqrt{\boldsymbol{p}_B^2 + m_B^2 + 2m_B V_B(r)} \sim m_B + \frac{\boldsymbol{p}_B^2}{2m_B} + V_B(r), \tag{6}$$

where $B = N$ or Y. These treatments enable us to include the potential effects naturally through the effective mass $m^{*2} = m_B^2 + 2m_B V_B(r)$. Consequently, the LOFA t-matrix have the dependence on the collision point r through nucleon and hyperon potentials, $V_B(r)$. It should be noted that the LOFA t-matrix is equivalent to ordinary optimal Fermi averaging t-matrix when potential effects are switched off. Product of incoming and outgoing distorted meson waves is evaluated in the eikonal approximation. In $(\pi^{\pm}, K^+)$ and (K^-, K^+) reactions at 1.20 GeV/c and 1.65 GeV/c, the isospin averaged cross sections are assumed to be $\bar{\sigma}_{N\pi^{\pm}}$=34mb, $\bar{\sigma}_{NK^+}$=18mb and $\bar{\sigma}_{NK^-}$=40mb, $\bar{\sigma}_{NK^+}$=30mb, respectively.

3 Results

3.1 Λ production spectrum

First, we calculate the Λ production spectrum using the well known parameters from the bound state spectroscopy, *i.e.* a typical depth of about 30MeV [2], in order to judge the validity of the present method.

In the calculation, we have assumed the one body Woods-Saxon type hyperon-nucleus optical potential,

$$U_Y(r) = (V_0^Y + iW_0^Y) f(r) + V_{ls}^Y \frac{\hbar^2 \boldsymbol{l} \cdot \boldsymbol{s}}{(m_\pi c^2)^2} \frac{1}{r} \frac{df(r)}{dr} + V_C^Y(r), \tag{7}$$

with $f(r) = 1/(1 + e^{\frac{r-R}{d}})$, $\quad R = r_0(A-1)^{1/3}$, where V_{ls}^Y and $V_C^Y(r)$ denote the spin-orbit strength and Coulomb potential, respectively.

Figure 1 shows the calculated results of Λ production spectrum ^{28}Si(π^+, K^+) at p_π=1.20 GeV/c, $\theta = 6^\circ$ in comparison with experimental data. The experimental data are taken from E438 at KEK. Solid line shows DWIA results with LOFA t-matrix with standard parameters $V_0^\Lambda = -32$MeV, $V_{ls}^\Lambda = 4$MeV, $r_0 = 1.1$fm and $d = 0.6$fm. We find good agreement of the calculated results with data in both of QF and bound state regions.

3.2 Σ^- production spectrum

DWIA analysis in the ordinary on-shell Fermi averaging t-matrix treatment can reproduce the (π^-, K^+) QF spectrum shape with the Batty's density dependent (DD) potential and Woods-Saxon potential with 30 MeV repulsion [8], but the absolute values are different in these calculations. It is desirable to describe the spectrum shape as well as the yield, and the LOFA t-matrix would be helpful for this purpose.

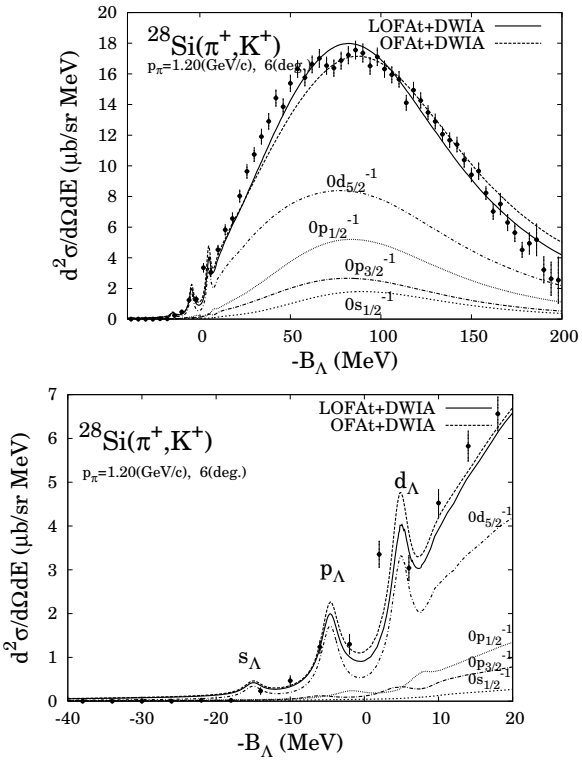

Fig. 1. The Λ hypernuclear production spectrum ^{28}Si(π^+, K^+) in the QF region (upper panel) and in the bound state region (lower panel) at p_π=1.2 GeV/c. Solid line shows LOFAt + DWIA results using Λ-nucleus potential depth of 32 MeV. Dotted line shows the Optimal Fermi Averaging t-matrix (OFAt) DWIA result. Other lines show hole contribution with 0s1/2, 0p3/2, 0p1/2 and 0d5/2, respectively, in LOFAt + DWIA.

In Fig.2, we show the Σ^- production QF spectrum ^{28}Si(π^-, K^+) at p_π=1.2 GeV/c. Calculated results using Woods-Saxon type optical potentials and Batty's DD potential [4] are compared with experimental data [6]. It turns out that experimental data on ^{28}Si target is reasonably well reproduced in Woods-Saxon type potential with small repulsion. In the Batty's DD potential, calculated result agrees with the experimental data in a wide excitation energy range. We can see the large potential dependence in the case of LOFAt + DWIA.

3.3 Ξ^- production spectrum

The depth of the Ξ^--nucleus potential has been suggested to be around 15 MeV from the analysis of the (K^-, K^+) spectrum in the bound state region [15]. In that analysis, the observed yield in the bound state region is compared with the calculated results, since the experimental resolution is not enough to distinguish the bound state peaks. Figure 3 shows calculated results of Ξ^- production spectra in LOFAt + DWIA with potential depth of 15 MeV in comparison with experimental data [16]. Calculated curves reproduce the experimental data systematically ,

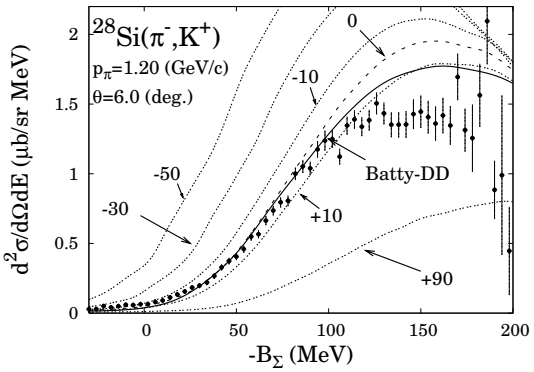

Fig. 2. Differential cross section of (π^-, K^+) reaction on ^{28}Si target at the incident momentum of p_π=1.2 GeV/c. The solid line shows result of Batty's DD potential with LOFAt + DWIA, Other line are calculated results with LOFAt + DWIA with potential depth of V_0=-50, -30, -10, 0, +10, +90 MeV(up to down), respectively. Imaginary part is fixed to be -20 MeV.

while the cross section at lower p_{K^+} region is underestimated, where the contribution from multistep processes is important [17].

In Fig. 4, we show the calculated K^+ spectrum in the bound state region of (K^-, K^+) reactions on ^{27}Al and ^{12}C targets with the same potential parameters $[(V_0^\Xi, W_0^\Xi) = (-15\text{MeV}, -1\text{MeV})]$ which explains the QF spectra. We have assumed an experimental resolution of 2 MeV. We find that bound state peaks are populated selectively as in the case of (π, K) reaction due to high momentum transfer, and these peaks can be identified if the experimental resolution is improved to be around 2 MeV.

4 Summary

We have studied hyperon-nucleus potentials through the QF spectra in (π^+, K^+) , (π^-, K^+) and (K^-, K^+) reactions using distorted wave impulse approximation (DWIA) with Local Optimal Fermi Averaging t-matrix (LOFAt) treatment. In addition to the on shell kinematics [9], nucleon and hyperon potential effects are included in the Fermi averaging procedure in LOFAt. We have found that LOFAt treatment is a better tool to describe the QF spectrum than standard Fermi averaging prescriptions. In comparison with the Λ production data, we find good agreement in both of QF and bound state regions with LOFAt + DWIA. From the comparison with the Σ^- production data, LOFAt + DWIA result prefers less repulsive Σ^- potential than those suggested in other theoretical models [8, 10]. This difference may come from the kinematics modification by the large difference in the initial (nucleon) and final (hyperon) state potentials. Finally, we investigate the Ξ^- production spectrum, and calculated results are found to be in good agreement with the experimental QF data using the Ξ^--nucleus potential depth of 15 MeV. We believe that the present modification would provide a better tool for the analysis of spectrum in the QF as well as the bound state region.

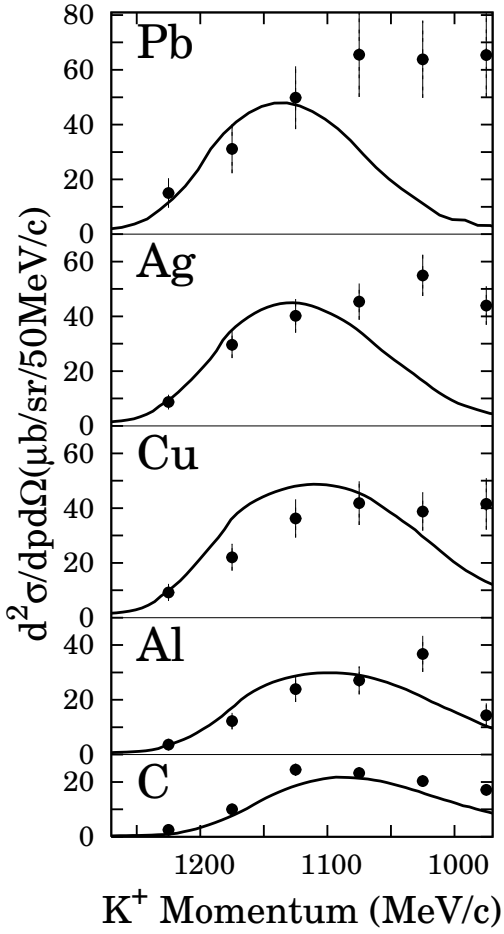

Fig. 3. The calculated Ξ^--hypernuclear production spectra in the QF region at p_π=1.65 GeV/c and 6(deg.) on C, Al, Cu, Ag and Pb targets in comparison with data [16]. Solid lines show LOFAt + DWIA results with $(V_0^{\Xi}, W_0^{\Xi}) = (-15\text{MeV}, -1\text{MeV})$, and the experimental resolution is assumed to be 10 MeV.

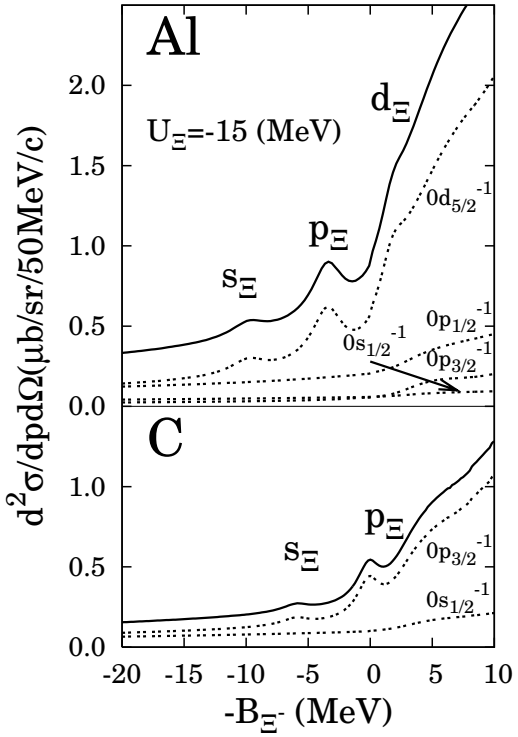

Fig. 4. The Ξ^--hypernuclear production spectrum in the bound region at p_π=1.65 GeV/c and 6 (deg.) on Al (upper panel) and C (lower panel) targets with LOFAt + DWIA. Potential parameters are used same as Fig. 3.

Acknowledgements

We would like to thank Prof. A. Gal, Prof. T. Harada and Prof. M. Kohno for valuable discussions. This work is supported in part by the Ministry of Education, Science, Sports and Culture, Grant-in-Aid for Scientific Research under the grant numbers, 15540243 and 1707005.

References

1. M. Kohno *et al.*, Nucl. Phys. A **674** (2000), 229.
2. D. J. Millener, C. B. Dover, and A. Gal, Phys. Rev. C **38** (1988), 2700.
3. T. Harada, S. Shinmura, Y. Akaishi and H. Tanaka, Nucl. Phys. A **507** (1990), 715; T. Harada, Phys. Rev. Lett. **81** (1998), 5287.
4. C. J. Batty, E. Friedman and A. Gal, Phys. Lett. B **335** (1994), 273; C. J. Batty, E. Friedman and A. Gal, Prog. Theor. Phys. Suppl. **117** (1994), 227; J. Mares, E. Friedman, A. Gal and B. K. Jenning, Nucl. Phys. A **594** (1995), 311.
5. R. H. Dalitz and A. Gal, Phys. Lett. B **64** (1976), 154.
6. H. Noumi *et. al.*, Phys. Rev. Lett. **89** (2002), 072301 [Erratum:Phys. Rev. Lett. **90** (2003) 049902.]; P. K. Saha *et. al.*, Phys. Rev. C **70** (2004), 044613.
7. N. Kaiser, Phys. Rev. C **71** (2005), 068201.
8. T. Harada and H. Hirabayashi, Nucl. Phys. A **744** (2004), 323.
9. T. Harada and Y. Hirabayashi, Nucl. Phys. A **767** (2006), 206; T. Harada and Y. Hirabayashi, Nucl. Phys. A **759** (2006), 143.
10. M. Kohno *et al.*, Prog. Theor. Phys. **112** (2004), 895.
11. E. H. Auerbach, A. J. Balitz, C. B. Dover, A. Gal, S. H. Kahana, L. Ludeking, and D. J. Millener, Ann. Phys. (NY) **148** (1983), 381.
12. O. Morimatsu and K. Yazaki, Nucl. Phys. A **483** (1988), 493; O. Morimatsu and K. Yazaki, Nucl. Phys. A **435** (1985), 727; T. Harada and Y. Akaishi, Prog. Theor. Phys. **96** (1996), 145; M. T. López-Arias, Nucl. Phys. A **582** (1995), 440.
13. S. Tadokoro, H. Kobayashi and Y. Akaishi, Phys. ReV. C **51** (1995), 2656.
14. B. W. Allardyce *et al.*, Nucl. Phys. A **209** (1973), 1.
15. T. Fukuda *et al.*, Phys. Rev. C **58** (1998), 1306. , P. Khaustov *et al.*, Phys. Rev. C **61** (2000), 054603.
16. T. Iijima *et al.*, Nucl. Phys. A **546** (1992), 588.
17. Y. Nara, A. Ohnishi, T. Harada, A. Engel, Nucl. Phys. A **614** (1997), 433.